Schweizerische Eidgenossenschaft
Confédération suisse
Confederazione Svizzera
Confederaziun svizra

Federal Department of the Environment, Transport, Energy and Communications DETEC

Swiss Federal Office of Energy SFOE
Energy Research and Cleantech

Final report dated 30.09.2022

UPero

Scale-up of perovskite solar cells

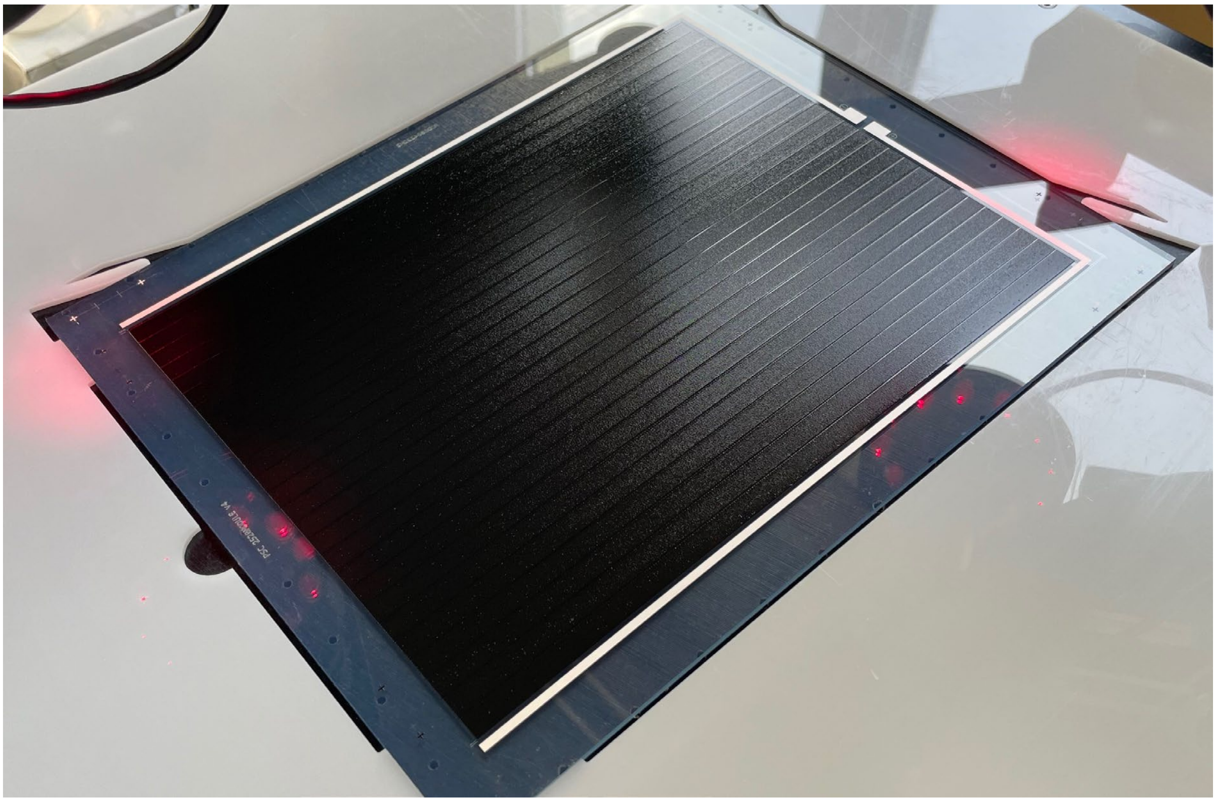

Source: @ Solaronix SA, 2022

Date: 30.9.2022

Location: Bern

Publisher:
Swiss Federal Office of Energy SFOE
Energy Research and Cleantech
CH-3003 Bern
www.bfe.admin.ch

Subsidy recipients:
Empa
Überlandstrasse 129
www.empa.ch

Solaronix SA
Rue de l'Ouriette 129
www.solaronix.com

Authors:
Frank Nüesch, Empa, frank.nueesch@empa.ch
Toby Meyer, Solaronix SA, toby.meyer@solaronix.ch

SFOE project coordinators:
Karin Söderström, karin.soederstroem@bfe.admin.ch
Stefan Oberholzer, stefan.oberholzer@bfe.admin.ch

SFOE contract number: SI/501816-01

Zusammenfassung

Die Hochskalierung der Kohlenstoff-basierten Perowskit Dünnfilmphotovoltaik Technologie (CPSC) stellt hohe Ansprüche an die Homogenität der photoaktiven Schichten über die gesamte Modulfläche. Das dreijährige Entwicklungsprojekt umfasst zunächst die Formulierung geeigneter Tinten sowie Prozessparameter zur Schlitzdüsen – und Siebdruckbeschichtung der porösen Multischichtstruktur auf 12.5 x 25 cm grossen Flächen. Ferner konnte mittels Tintenstrahldruck ein Verfahren entwickelt werden, um das metallorganische Halidsalz gleichförmig auf die poröse Schicht aufzutragen. Mit dem Ziel, effiziente Module herzustellen, wurde die monolithische Serienschaltung mittels Laserablation und Präzisionssiebdruck erreicht. Nach Optimierung der Prozessparameter konnte die Zieleffizienz von 13% auf 57.6 cm^2 grossen Modulen erreicht werden. Schliesslich wurde ein Einkapselungsverfahren entwickelt und ein Feldtest mit einem Modul einer Fläche von 518 cm^2 durchgeführt. Besonders hervorzuheben ist, dass die Fabrikation der Module in gewöhnlicher Luft ausgeführt wird, und dass die monolithische Verschaltung von Zellen zu einem Modul verlustfrei erfolgt. Das Projekt führte ausserdem zu mehreren Publikationen, zwei Patenten, zahlreiche Pressemitteilungen und der Gründung einer Start-up.

Résumé

La mise à l'échelle de la technologie photovoltaïque en couches minces à base de pérovskite (CPSC) exige une grande homogénéité des couches photoactives sur toute la surface du module. Le projet de développement de trois ans comprend tout d'abord la formulation d'encres appropriées et de paramètres de processus pour l'enduction par buse à fente et par sérigraphie de la structure multicouche poreuses sur des surfaces de 12.5 x 25 cm. En outre, un procédé d'impression à jet d'encre a été mis au point pour appliquer uniformément l'halogénure organométallique sur la couche poreuse. Dans le but de fabriquer des modules efficaces, la connexion en série monolithique a été réalisée par ablation laser et sérigraphie de précision. Après optimisation des paramètres du processus, l'efficacité cible de 13% a pu être atteinte sur des modules de 57,6 cm^2 de surface utile. Enfin, un procédé d'encapsulation a été développé et un test sur le terrain a été réalisé avec un module d'une surface utile de 518 cm^2. Il convient de souligner que la fabrication des modules est réalisée dans l'air ordinaire et que l'interconnexion monolithique des cellules en un module se fait sans perte. Le projet a en outre donné lieu à plusieurs publications, deux brevets, de nombreux communiqués de presse ainsi que la création d'une start-up.

Summary

The scale-up of the carbon-based perovskite thin-film photovoltaic technology (CPSC) places high demands on the homogeneity of the photoactive layers over the entire module surface. The three-year development project includes the formulation of suitable inks as well as process parameters for slot-die coating and screen-printing of the porous multilayer structure on 12.5 x 25 cm surfaces. Furthermore, by means of inkjet printing, a process could be developed to apply the metal-organic halide salt uniformly onto the porous layer. With a view to producing efficient modules, monolithic series connection was achieved by laser ablation and precision screen printing. After optimising the process parameters, the target efficiency of 13% was achieved on modules with aperture area of 57.6 cm^2. Finally, an encapsulation process was developed and a field test was carried out with a 518 cm^2 aperture large module. Particularly noteworthy is that the fabrication of the modules is carried out in ordinary air, and that the monolithic interconnection of cells to form a module is loss-free. The project also led to several publications, two patents, numerous press releases and the launch of a start-up.

Take home messages

- A very efficient mass manufacturing line could be envisaged using industrially well established slot-die coating and laser scribing equipment. The two patented slot-die deposition processes regarding slot-die deposition of all active layers as well as the “all-in-one” curing cycle allow for very fast active layer coating.

- Scale-up of CPSC perovskite solar cells on large area is straight forward. Due to the porous nature of the mesoscopic scaffold, crystallization of the infiltrated perovskite ink occurs uniformly all over the surface.

- Monolithic interconnection of CPSC perovskite solar cells is loss free. The CPSC architecture benefits from the fact that the relevant laser scribes (P1, P2 and P3) occur before infiltration of the active perovskite ink material.

- CPSC perovskite solar cell fabrication can be carried out in regular industrial atmosphere. This obviates the need for clean room or protected atmosphere.

- The CPSC devices proved to be very efficient at low light conditions, making them suited for specialty applications like powering electronic goods, sensors, and other internet-of-things related devices. The industrially relevant production techniques developed within UPero come in handy to address this specific market.

Contents

Abbreviations

CPSC	Carbon based perovskite solar cell
HTL	Hole transport layer
ETL	Electron transport layer
TCO	Transparent conducting oxide
FTO	Fluorine-doped tin oxide
c-TiO_2	Compact TiO_2 layer
m-TiO_2	Mesoporous TiO_2 layer
m-ZrO_2	Mesoporous ZrO_2 layer
PCE	Power conversion efficiency
PV	Photovoltaic
SCP	Screen printing
SDC	Slot-die coating
SUPSI	University of Applied Sciences and Arts of Southern Switzerland
Voc	Open circuit voltage
P1, P2, P3	Laser scribing steps used for module fabrication
F-ISE	Fraunhofer Institut für Solare Energiesysteme

1 Introduction

1.1 Background information and current situation

The advent of hybrid perovskites in the family of solar cell technologies is spurring tremendous research activities worldwide. The major thrust for endorsing this thin film technology consists of the competitive power conversion efficiencies exceeding 25.7 %[1], low manufacturing costs and interoperability with well-established technologies such as crystalline silicon and CIGS. Following the huge research effort with thousands of scientific publications every year, industrial implementation has gained impetus. [2-7]

To date the largest certified perovskite PV module reaches an efficiency of 17.9 % [8] for an active area of 800 cm^2, while for smaller areas > 30 cm^2 efficiencies of 20.8% were reported. [4] The performance difference between laboratory champion cells and modules has therefore shrunk significantly, illustrating the great advances this solar cell technology has made in recent years. [9] In order to reduce production costs, wet deposition fabrication is most promising with appealing prices of 3-5 cts/W$_p$ for high throughput lines. [10] However, scale-up comprises several challenges among which large area coating using industrial processes, module segmentation and interconnect strategy as well as encapsulation. [11]

Achieving homogenous film stacks over a large area is a difficult task, particularly for the small film thicknesses used in perovskite technology. Pinholes or defects created by foreign particles may annihilate all efforts put into module fabrication. In a production line, this issue can easily bring the fabrication yield below unity, which in most cases implies strict inert atmosphere and clean room conditions. Homogeneity of the active PV stack over a large surface also means unchanged electronic and interface properties between the layers. There are numerous effects that could lead to variations of these properties, e.g. crystallite size of the absorber layer, grain boundary passivation and interface formation. For wet deposition processes it is clear that homogeneous drying has to be mastered as well. [5,12]

Interconnect strategies are necessary because the transparent electrode naturally has limited conductivity as compared to a plain metal layer. Large area cells would produce high electrical current and major resistive loss. While applying a metal grid would cope with such losses, it also would reduce the active surface of the cell. [11] Therefore the common strategy consists of segmenting the large surface into stripes of < 1cm which are connected in series. Among the various approaches, monolithic interconnection using P1, P2 and P3 scribes is the most advantageous in terms straightforward fabrication steps and reduced loss of active surface.

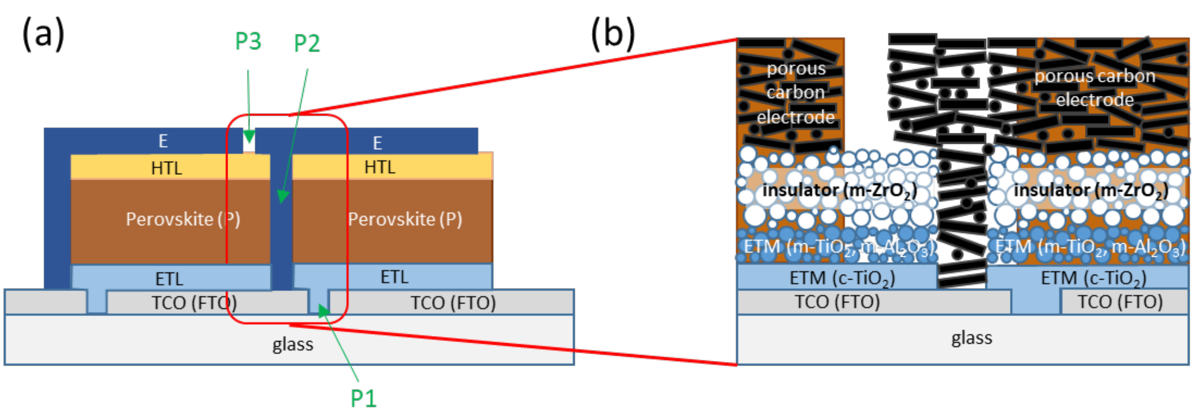

Figure 1 Monolithic interconnect structure commonly used in thin-film photovoltaic technologies indicating the electron transport layer (ETL), the hole transport layer (HTL), the electrode (E) as well as

the laser scribes P1, P2, P3 (a). Benefitting from the particular carbon-based perovskite solar cell (CPSC) structure and fabrication mode, an idealized interconnect can be designed (b).

As illustrated in Figure 1a such interconnect also introduces a new contact between the electrode E and the absorber material P (see red circular line) which may lead to either a chemical reaction and add recombination sites. Furthermore, laser processing locally heats up the substrate and the active layers leading to local thermal damage. In this project we are using the so-called carbon-based mesoscopic perovskite solar cell (CPSC) architecture which is a superstrate orientation with the following stack sequence: glass/FTO (400 nm)/c-TiO_2 (50 nm)/m-TiO_2 (500 nm)/m-ZrO_2 (1000 nm)/carbon (12 microns). This particular structure bears several advantages with respect to above mentioned scale-up challenges. If the porous oxide and carbon layers can be deposited homogeneously over a large surface, the infiltrated perovskite absorber has to accommodate within the sintered scaffold, which eliminates large grain formation. Infiltration occurs only after sintering the full stack structure meaning that laser scribing can first be applied to the empty oxide and carbon scaffold before infiltrating the perovskite ink. The latter is therefore neither affected by the laser beam nor by the carbon layer, which fills the gap created by the P2 scribe (see Figure 1b). By circumventing these characteristic issues of scale-up, CPSC promise a smoother transition from small area cells to large area modules. Eventually, it has to be noted that all CPSC fabrication can be carried out in normal atmosphere greatly reducing investment costs.

1.2 Purpose of the project

The purpose of this project is to demonstrate the feasibility of perovskite module production using industrially relevant high feedthrough processes such as slot-die coating, screen printing and laser scribing. The solar module stacks investigated here belong to the so-called carbon-based perovskite solar cells (CPSC) and shall be tested for their reliability under artificial and natural aging conditions. The project shall foster our competences in coating and solar-module manufacturing to achieve a high level of competence on an international level. This will allow us to participate in future international consortia, such as those funded by the EU framework program. The developments aimed in this project shall as well generate and support future entrepreneurial activities in this field in Switzerland. It is also intended to federate Swiss efforts in this field and to launch future development activities in a larger consortium.

1.3 Objectives

Given the enormous challenges we faced within a tight timeframe (partly also imposed by the Corona-virus epidemic), it appeared unrealistic to produce an optimized large area module of 12.5 x 25 cm with high efficiency. Therefore, the efforts were directed towards demonstrating the technical feasibility of large area CPSC module fabrication by demonstrating four crucial steps, necessary to be mastered before tackling a full size module:

- Homogeneity of large area stack surface probed by local PV performance
- Monolithic Interconnect by laser ablation
- Efficiency improvement using the salt additive approach
- Encapsulation and stress testing
- Fabrication of a demonstrator and field testing

During the three years of the project the collaboration between Empa and Solaronix was very strong and implied a clear task sharing. There were regular short and long visits by the key scientists involved in the project. At the end of the project, an Empa scientist moved to Solaronix and launched his own start-up.

Homogeneity of large area stack surface

Layer homogeneity over a large area is one of the most challenging milestones to reach in scale-up. This comprises of course morphological and structural homogeneity such as layer thickness and film continuity, which were achieved during phase I and proven using optical and electron microscopy, scanning force microscopy as well as profilometry. Furthermore, homogeneous infiltration over the full surface must be mastered. This was also achieved during phase I using inkjet printing and given the very promising results, Solaronix decided to purchase a Pixdro LP50 inkjet printer (SUSS Microtec). The printer was commissioned at the end of the first project year and allowed Solaronix to infiltrate large area CPSCs in an extremely homogeneous way (from a business point of view, mastering this process at Solaronix opened new perspectives and generated an industrial mandate). None of above mentioned inspection methods, however, are able to assess the quality of the semiconducting properties or interfaces of the stack structure. For this reason a method had to be sought that can measure the photovoltaic performance locally on the large area plate. Ideally, a full scale module can be built, necessitating monolithic interconnect structure, which is indeed the final goal of the project. To assess the large area coatings in a more efficient way, individual cells were fabricated on various square spots of the large multilayer stack area and measured individually. Phase II of the project allowed to develop and assess optoelectronic homogeneity of over a 12.5 x 25 cm large area.

Interconnect technique

During phase I of the project, different strategies to interconnect the individual cells of the module were evaluated. Two parallel routes were pursued, namely additive and subtractive methods. The additive method consisted of precision screen printing with the possibility to define thin lines of a couple hundreds of microns. This technique was further developed in the second year, by including lift off for one of the stack layers. Regarding subtractive structuring, we opted for a laser scribing process and purchased a TruMark station 5000 nanosecond pulsed UV laser from Trumpf, which became operative at the beginning of the second project year. A major part of the efforts was devoted to achieving P2 scribing, due to the fact that it is difficult to ablate the c-TiO_2 layer, which is sandwiched between the readily ablatable mesopourous and FTO layers. During P2 scribing the 50 nm thin c-TiO_2 layer has to be ablated completely without deteriorating the underlying FTO layer.

Efficiency improvement

Based on the promising results obtained during phase I of the project by adding large amounts of salt to the perovskite ink, we decided to scrutinize salt additives in more depth. Based on recent papers, we also attempted to change the perovskite ink stoichiometry by adding additional organic and metal cations and by using mixed chloride and bromide halide anions. Yet a third attempt consisting of passivating the TiO_2 emitter layer was undertaken. The objective was to identify a clear direction to follow for raising efficiency in CPSC perovskite solar cells.

Encapsulation and stress testing

Encapsulation and stress testing are crucial to the demonstration of a viable PV technology. It was planned to carry out this task in collaboration with our partners at SUPSI (Canobbio). Testing at the cell level, however, is not effective at their premises and therefore we teamed up with colleagues at the Fraunhofer ISE in Freiburg i. B. Advantageously, Solaronix has a running EU project including a partner laboratory at F-ISE. This channel could be used to run stress tests on a number of different encapsulation strategies. Additionally, a collaborator contract was signed between Empa and the MetroPV consortium including another laboratory at F-ISE being interested to test lifetime on our encapsulated cells. Finally the possibility to stress test CPSC with an external industrial customer was adopted. Testing of modules will be carried out in the future, once the field tests provide positive results.

Demonstrator and field testing

Module fabrication took place during phase II and proceeded during the third year of the project. The main challenges were to adapt laser scribing with an available optical control of about 5 x 5 cm to a combined optical and mechanical control allowing to process much larger surfaces up to 30 x 30 cm. Alternatively, precision screen printing was further refined to reduce the non PV-active interconnect area to as much as 4%. This process was finally adopted to fabricate 7.6 x 7.6 cm aperture modules segmented into 12 cell stripes. Modules were encapsulated with a top glass cover laminated by a polyolefin film and provided with a junction box. A total of 9 such modules were then connected in parallel to build the demonstrator used to power a weather station on the rooftop of the NEST building at Empa. Due to delays caused by the Covid pandemics and the lack of personnel to carry out all project tasks with the necessary depth, a half year prolongation was requested.

2 Procedures and methodology

2.1 Large area slot-die coated CPSC (WP2)

In order to accelerate the development, we decided to merge the investigation of PV response homogeneity of the large area stack and the interconnect strategy in a single experimental approach. The latter consisted of slot-die coating a full stack structure on a large area 12.5 x 25 cm conductive oxide (FTO) substrate and subsequently segment it into squares of 1.4 x 1.4 cm. The latter squares can either be tested as single cells or can be split into two for developing interconnection (dual cells). A corresponding scheme is shown in Figure 2. The workload was shared in the following way. Solaronix provided large area FTO coated glass substrates already featuring P1 scribing lines. Empa then applied slot die coating of all the oxide layers and carried out P2 scribing, except on areas dedicated for reference cells. Samples were then shipped back to Solaronix for screen-printing carbon on top of the cell segments. In order to focus on the P2 scribing only, we decided to segment the carbon top electrode by screen printing. After firing the segmented carbon layer, the perovskite ink was infiltrated into the individual cell stacks using the inkjet protocol developed during Phase I of UPero. The technology necessary for the infiltration step has been successfully transferred to Solaronix and therefore infiltration was carried out at Solaronix. The standard cell fabrication procedure included a standard heat/damp post treatment, which was applied to both single and dual cells on the test substrate. Pursuing this strategy, the quality of the active device stack layers was assessed by:

- Optical and electron microscopy analysis of homogeneity and thickness
- Characterization of test devices

2.2 Interconnect methods (WP2)

The nanosecond pulsed UV (355nm) laser from Trumpf has been purchased and commissioned at Empa. In parallel additive structuring methods, i.e. using precise screen-printing, were addressed. These tasks encompassed the following points:

- Elaborating laser processing parameters for P2 and P3 scribing
- Exploring additive interconnect strategies
- Characterization of laser ablated patterns using optical microscopy and profilometry
- Defect analysis using thermography and electroluminescence imaging
- Assessment of scribe quality by manufacturing dual cells

2.3 Efficiency hunting

Based on promising results obtained during the last year using salt addition to the perovskite ink, a more systematic study was carried out:

- Addition of various lithium salts to the perovskite ink: LiF, LiCl , LiBr, LiI
- Passivation of the TiO_2 surface using silanes and phosphonates
- Quadruple cation perovskite inks: $(FAPbI_3)_{83}(MAPbBr_3)_{17}$ + CsI+RbI

2.4 Encapsulation

Various approaches have been tested amongst which ionomer and polyolefin encapsulants for glass/glass encapsulation.

2.5 Stress testing

Stress tests were carried out in collaboration with the European consortium MetroPV. Empa signed a collaborator contract with the latter. Numerous testing cells have been shipped by Solaronix SA and are currently tested at F-ISE. The devices however, were not stress tested as planned. The European consortia were first trying to find standard procedures to measure simple current-voltage curves at room temperature. This alone proved to be a major challenge due to the significant hysteresis loop of modules and cells. Therefore stress testing was carried out with one of our industrial customers on encapsulated cells. Field testing of the first encapsulated modules showed severe deficiencies and therefore it was decided to test modules at SUPSI once the encapsulation has attained better performance.

2.6 Demonstrator fabrication

At the end of phase II of the project, scribing and coating processes allowed us to fabricate modules reproducibly with an active area of about 57.6 cm^2. The strategy was therefore pursued to encapsulate such modules individually and to provide a junction box to each of them. 9 of these modules were then connected in parallel to produce a demonstrator module with an active area of 518 cm^2.

3 Activities and results

3.1 Large area CPSC stack coating (WP1 and WP2)

The slot-die coating equipment at Empa was adapted to accommodate substrate sizes of 12.5 x 25 cm. The inks and slot-die coating parameters were adjusted to achieve homogeneous wet film thicknesses. Slot-die coating can handle inks within a wide viscosity window ranging from 1 mPas to 10,000 mPas[13]. For a successful coating, it is mandatory that a stable meniscus is formed between bead and substrate. This can be predicted and consolidated with the help of critical capillary numbers. Figure 2a shows the critical capillary number as function of film thickness. For higher capillary numbers the coating bead becomes unstable. For example, due to the low film thickness of c-TiO_2, slot-die coating at that speed is close to the critical value and may not allow increasing the coating speed further. Besides, also substrate wettability can be quantified with the help of wetting envelopes that guides the choice of solvents (Figure 2b).

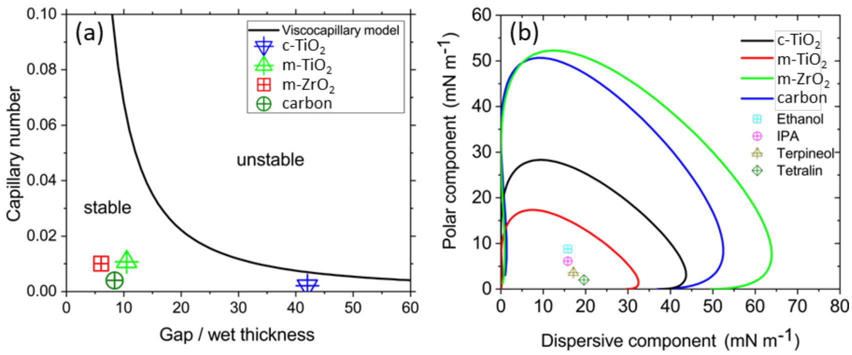

Figure 2: (a) Critical capillary number and capillary numbers of slot-die inks as function of wet film thickness. (b) Wettability envelope of the individual layers of a CPSC solar cell and surface energies of solvents used for ink formulation.

We were able to scale-up slot-die coating of all five layers of the CPSC stack (Figure 3).

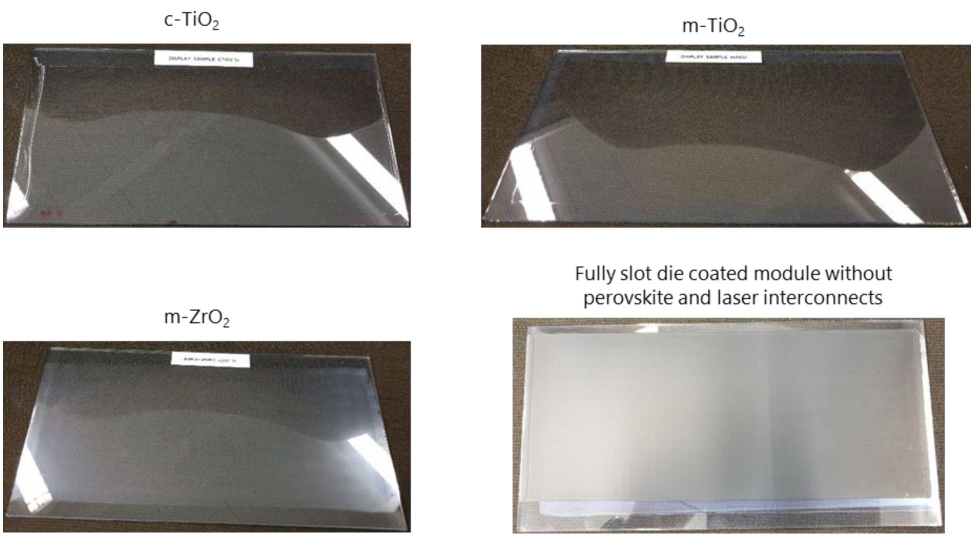

Figure 3: Large area slot-die coating of all oxides used in the CPSC stack on 12.5 x 25 cm substrates. The wet films were dried at 70 °C (c-TiO_2) or 110 °C (all other oxide layers). After depositing the carbon layer, the films were fired at 500 °C for 30 minutes.

Conventional infiltration of perovskite precursor ink occurs via semi-automatic pipetting depositing a certain droplet volume onto the layer (Figure 4a). This method is however not precise enough to homogeneously fill the porous multilayer stack. The excessive liquid volume in the droplet center swells up part of the carbon electrode. Therefore, we developed the possibility of controlled drop on demand infiltration of the precursor ink using inkjet printing at Empa (Figure 4b) to fine-tune the printing parameters.

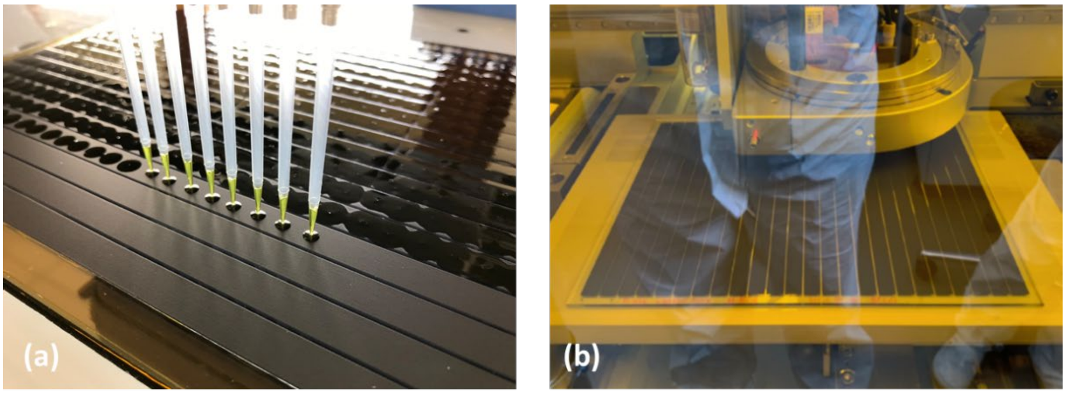

Figure 4: Automatic dispensing of perovskite precursor solution (a). Inkjet infiltration of the CPSC module (b)

Careful adjustment of jetting parameters, drop density, drop volume and number of passes allows reaching the same power conversion efficiencies as for pipetting. As inferred from X-ray diffraction analysis, post-infiltration crystallization of the organo-metal halide perovskite proceeds as well as for the other infiltration methods. Furthermore, inkjet is much more precise, uses a lower perovskite volume of 5 µL to 3 µL, thus reducing the lead content (Table 1). At the same time this printing method avoids spilling, it can be used in a controlled environment to avoid lead contamination and allows a rather large window for the processing parameters. Perhaps the most important merit consists of industrial scale-up capability as we have developed the process using industrial printheads (Konica Minolta KM512).[6]

Table 1: Power conversion efficiency of 1.5 cm^2 area CPSC devices as a function of inkjet printing parameters (number of passes, total ink volume and substrate temperatures.

Number of passes	Ink volume (µL)	Substrate temperature(°C)	PCE (%) Reverse	PCE (%) Forward	PCE (%) Average
1x	1,5	25	1.4	1.4	1.4
2x	3	25	13.1	11.5	12.3
3x	4.5	25	13.1	12	12.5
1x	6	25	8.8	7.3	8
1x	6	50	8	7.2	7.6

In order to accelerate CPSC development, we decided to merge the investigation of PV response homogeneity of the large area stack and the interconnect strategy in a single experimental approach. The latter consisted of slot-die coating a full stack structure on a large area 12.5 x 25 cm conductive oxide (FTO) substrate and subsequently segmenting it into squares of 1.4 x 1.4 cm. The latter squares can either be tested as single cells or can be split into two for developing interconnection (dual cells). Solaronix provided large area FTO coated glass substrates already featuring P1 scribing lines. Empa then applied slot-die coating of all the oxide layers and carried out P2 scribing, except on areas dedicated for reference cells. Samples were then shipped back to Solaronix for screen printing carbon on top of the cell segments. In order to focus on the P2 scribing only, we decided to segment the carbon top electrode by screen printing. After firing the segmented carbon layer, the perovskite ink was infiltrated into the individual cell stacks using the inkjet protocol developed during Phase I of UPero. The technology necessary for the infiltration step has been successfully transferred to Solaronix and therefore infiltration was carried out at Solaronix. The standard cell fabrication procedure included a standard heat/damp post treatment, which was applied to both single and dual cells on the test substrate.

A convenient structuring method was to mask the edges of individual cells using tape prior to slot-die coating. After this initial solution we used laser ablation to remove redundant oxide and carbon layers. The laser parameters had to be adjusted accordingly (so-called hatching process). This yielded a highly precise edge definition as shown in Figure 5. The same process parameters were used to define 36 cells on the 12.5 x 25 cm substrate, which was subsequently cut into two plates, each containing 18 cells.

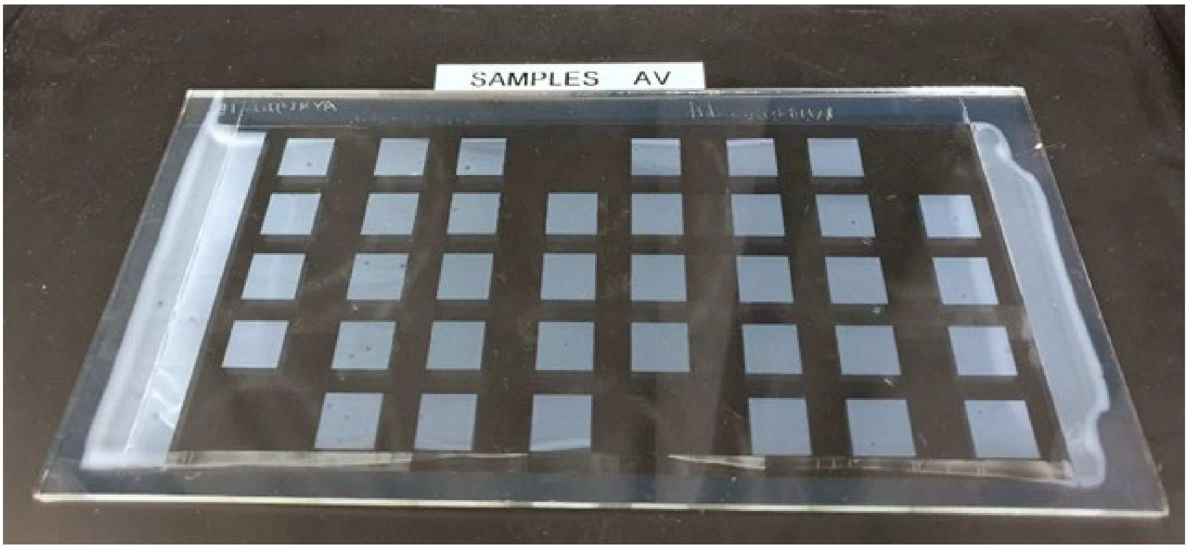

Figure 5 Picture of all oxides slot-die coated on FTO coated glass substrate of 12.5 x 25 cm with laser hatching for edge definition. The sample contains reference single cells as well as dual cells

The accelerated development strategy to process single (reference) as well as dual cells (interconnected in series) on large area substrates allowed to test layer homogeneity and interconnect quality at the same time. Albeit being efficient, the workflow required for a typical device testing cycle is quite labor intensive and lengthy (Figure 6).

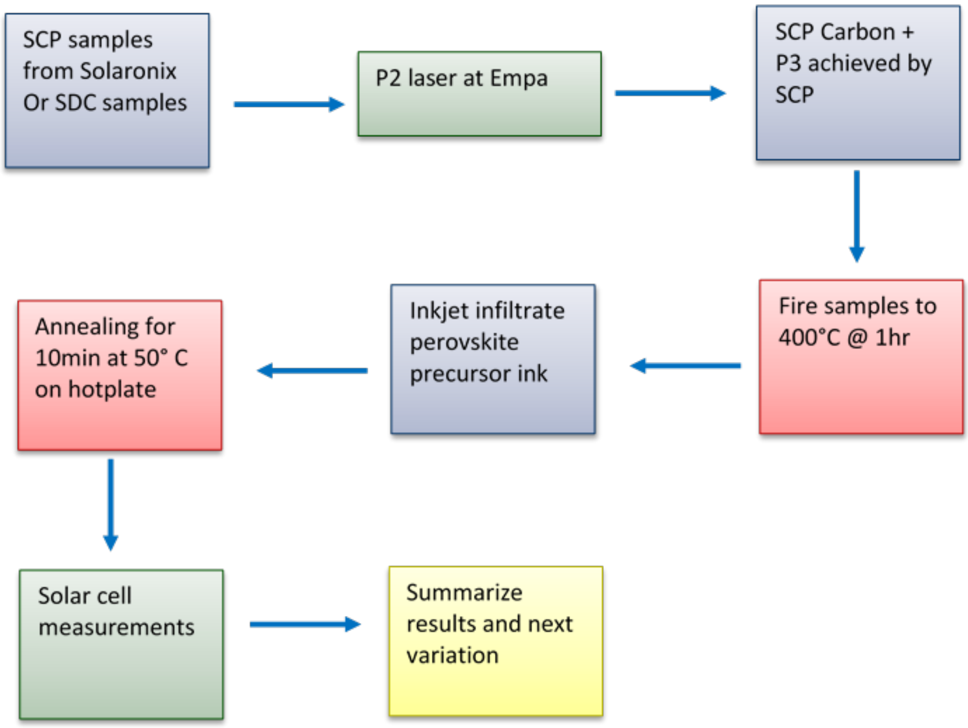

Figure 6 Typical workflow diagram to test P2 ablation of MPSC. SCP stands for screen printing, SDC for slot-die coating

3.2 Interconnect method (WP2)

A typical interconnect scheme for a dual cell is displayed in Figure 1. The laser parameters were developed to obtain P1 ablation of FTO to separate the two cells. P2 was developed to separate two individual cells by removing all the metal oxides and without removing the FTO. This was indeed the main focus since removal of the 50 nm c-TiO_2 turned out to be very challenging. Figure 7a shows a confocal scanning optical microscopy image of P1 and P2 scribes where the trace (Figure 7b) is taken along the arrow direction. We demonstrated that P3 could also be obtained using the same laser (Trumpf TruMark station 5000). However, in order to be able to focus solely on the quality of the P2 scribe, we deposited corresponding carbon electrode patterns by precision screen-printing. Figure 7c shows an optical microscopy image of perfectly aligned P1, P2 and P3 with a non-active gap created by the interconnect of 560 µm. When scribing larger surfaces, alignment of the P1, P2, and P3 becomes critical because misalignments can create short circuits.

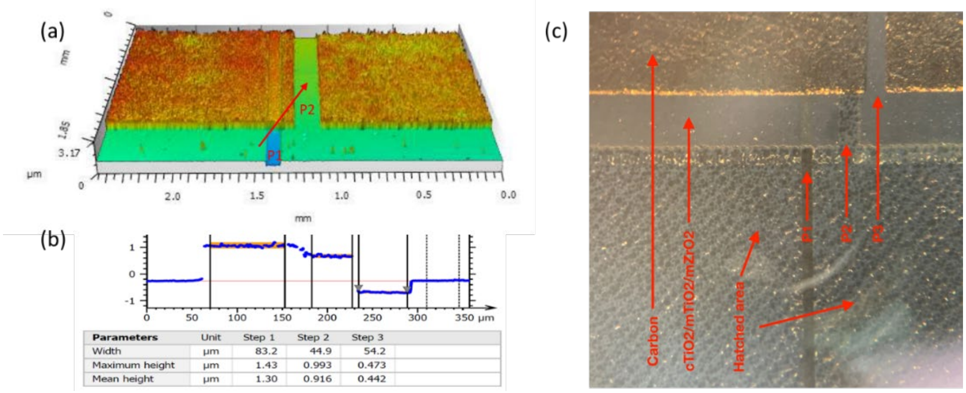

Figure 7 Typical P1 and P2 scribing pattern alignment characterized by confocal optical microscopy (a). The high profile (b) was taken along the direction of the red arrow in a. Optical microscopy image of the interconnect structure including the screen-printed carbon electrode. The length of the frame is 2 mm (c).

P1 scribing

The P1 insulation line is responsible for segmenting the FTO into stripes of about 6 mm in width. Scribing can be done at Solaronix using an NIR fiber laser as well as at Empa using the pulsed UV laser. The Trumpf laser at Empa has a marking field of 80 mm, which means it can mark a line or area of a maximum of 80 x 80 mm without moving the sample. The sample holder of the laser table, however, is equipped with a translation stage allowing covering surfaces of 30 x 30 cm. The laser is furthermore equipped with an imaging system that detects the scribing lines and can be programmed such that a smooth connection between different stitching areas is guaranteed (Figure 8).

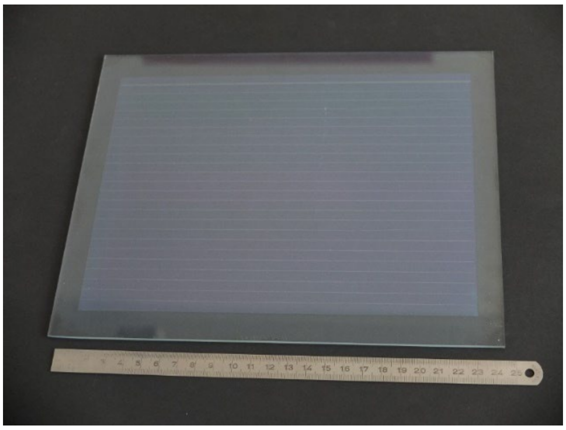

Figure 8 Large area 16.3 x 21.3 cm oxide stack deposited by screen-printing showing P2 scribing lines. P1 scribing was also carried out on this samples, but the lines cannot be seen on the figure.

P2 scribing

To get a good P2 scribing for monolithic interconnection, all the metal oxides, i.e. c-TiO_2, m-TiO_2, m-ZrO_2, need to be removed selectively without damaging the FTO underneath. We observed that it was fairly easy to ablate the nano-porous layers of m-TiO_2 and m-ZrO_2. To assess ablation of the 50 nm c-TiO_2, however, profilometry, con-focal microscopy, resistivity, SEM-EDX, were found to be not precise enough to determine the level of $c\text{-}TiO_2$ removed. We proceed with two further approaches to measure the presence of $c\text{-}TiO_2$. The first one consists of measuring the contact resistance (see Figure 1b) on the carbon landing area (this is the area where carbon touches FTO. If we intentionally coat FTO with $c\text{-}TiO_2$ and thereafter remove it with the laser and deposit carbon, we can measure the contact resistance). This is a large area though and it is necessary to do a similar experiment with the area in the P2 scribe, which we did by varying the P2 gap width and measuring the J-V curve. With these experiments we could prove that the presence of $c\text{-}TiO_2$ in the P2 scribe has a direct effect on the shape of the IV-curve: a so-called "S-shape" is appearing. By, reducing the laser pulse frequency to 45 kHz from 55 kHz we were able to ablate $c\text{-}TiO_2$ as can be deduced from the scan profile below (see Figure 9). To make sure that $c\text{-}TiO_2$ is properly removed, the following laser parameters were tuned: power, frequency, scribe velocity, and line width (see Table 1).

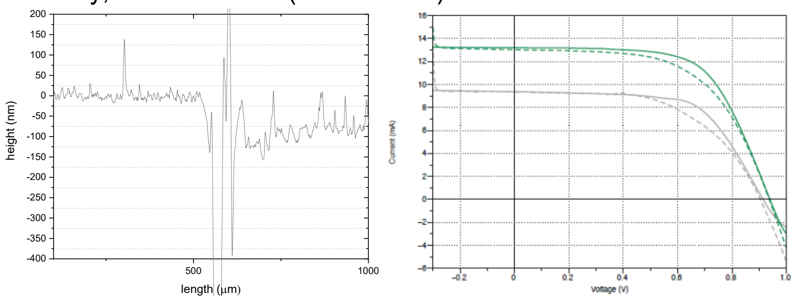

Figure 9 Height step induced by P2 scribing of 50 nm $c\text{-}TiO_2$ (left). IV characteristics of a reference cell, where the carbon-FTO contact (carbon landing area) was freed from an initial $c\text{-}TiO_2$ coating using pulsed laser ablation. Forward (plain line) and reverse (dashed line) scans are indicated for fresh (grey) and incubated (green) cells.

In order to allow comparison with screen-printed (SPC) reference devices, we first used screen-printed dual cells for P2 scribing development. It was possible to achieve dual cells, which achieved efficiencies of around 13%, similar to the value obtained for reference cells (see Table 2). A detailed overview of a typical batch investigation is given in the appendix, including four scans as well as optical microscopy images of the interconnect scribing lines. By means of this analysis it could be clearly seen that the reduced performance for some of the devices is due to misalignment of the scribing lines.

Table 2 Summary of the dual cell performance with the P2 laser process development. Cells were fabricated by screen-printing. The total active area was 14 x 14 mm and a 8 x 8 mm aperture mask was used for all cells.

Sample	Power	Frequency (Hz)	Velocity	Width (mm)	Voc (V)	Jsc (mA/cm^2)	FF (%)	Efficiency (%)
Trial 1	85%	85k	400	0.1	1.6	7.4	57	7.15
Trial 2	95%	60k	3000	0.1	1.75	8.0	57.6	8.1
Trial 3	100%	60k (2x)	3000	0.2	1.56	9.76	54.5	8.3
Trial 4	100%	55k	3000	0.2	**1.79**	5.6	**58.3**	**11.35**
Trial 5	100%	45K	3000	0.35	**1.84**	9.9	**72.9**	**13.2**
Trial 6	100%	45K	3000	0.2	**1.93**	9.5	**65.8**	**12**

Slot-die coated (SDC) device stacks could be successfully scribed using the same laser parameters as for SPC devices. Slot-die coating of all oxides was done stepwise on a 12.5 x 25 cm FTO glass, following standard coating and drying parameters. The samples were fired stepwise. To obtain single or dual cell segments on the substrate, the non-active slot-die coated areas are removed using the laser (hatching procedure) allowing the carbon to touch the FTO on the cathode side. Hatching of the area and P2 line to make the dual cells can be done individually or together. The laser parameters from Table 2 (Trial 4) were used for hatching and as well as for the P2 line.

Table 3 Summary of the performance of single and dual cells fabricated by slot-die coating where the solar cell segments of 1 x 1 cm (aperture, total area 1.4 x 1.4 cm) were defined by hatching. Cells were incubated.

Device		Voc (V)	Jsc (mA/cm^2)	Fill factor (%)	Efficiency (%)	Aperture area (cm^2)
Single-cell 1	Rev	0.87	16.4	37.7	5.40	1
	Fwd	0.87	16.4	38	5.42	1
Single-cell 2	Rev	0.91	15.4	33	5.8	1
	Fwd	0.91	15.6	32	5.8	1
Dual cell 1	Rev	1.73	6.95	46.7	5.6	1
	Fwd	1.73	6.96	47	5.6	1
Dual cell 2	Rev	1.83	5.5	50	5.1	1
	Fwd	1.84	5.5	52.04	5.3	1

The slot-die coated samples with dual cells were measured at Solaronix, and summarized in Table 3 above. The samples received Carbon top electrode by SPC with P3 and the next steps as per workflow reported in Figure 6. These samples have a 100 µm P2 with a gap of 100 µm. The alignment was done manually. Dual cells fabricated by slot-die coating yielded modest efficiencies of 5.6% with a Voc of 1.73 V for an aperture area of 1 cm^2 (see Table 2 below). However, it appears that single cells have a similar PCE efficiency. Both cells suffer from a low fill-factor, which must be further investigated. One origin of performance loss in solar cells are shunts and point defects. Similarly, resistive losses along the scribing connection are of concern.
Thermography and EL imaging studies were carried out in collaboration with the group of Prof. Beat Ruhstaller at ZHAW. Comparison with SPC devices revealed a stark contrast to SDC devices (Figures 10-12).

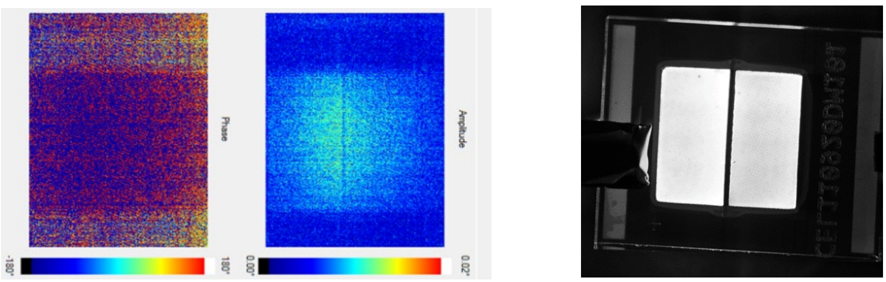

Figure 10 Dual cell Solaronix (screen-printing). Left: Dark lock-in thermography (DLIT) at 4 V. The cells only heat up at higher voltage, but then homogeneously. Right: EL in these cells at 2.4 V (onset).

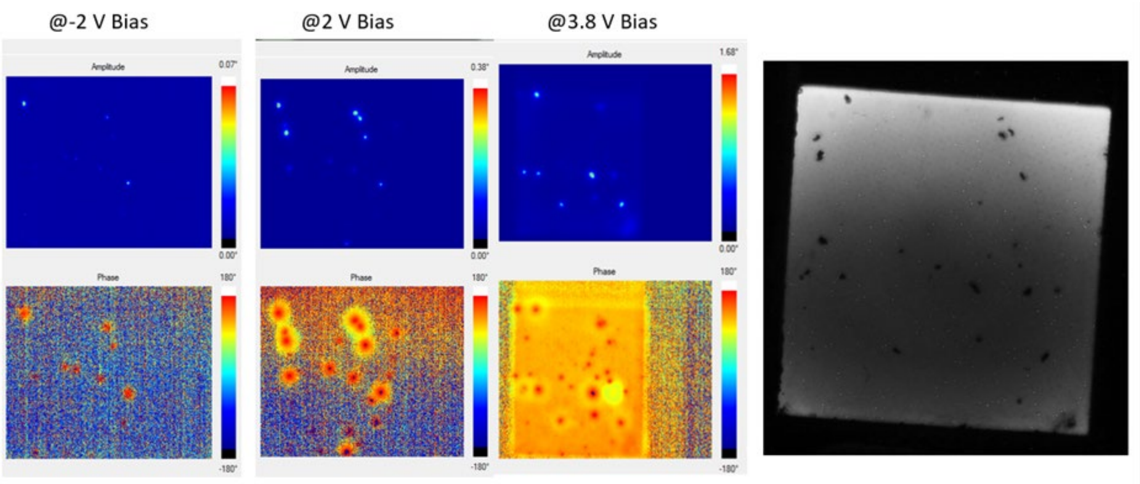

Figure 11 Empa reference cells (slot die coated MO layers, laser hatching, screen printed Carbon layer. Both DLIT and EL images show hot spots at higher voltages.

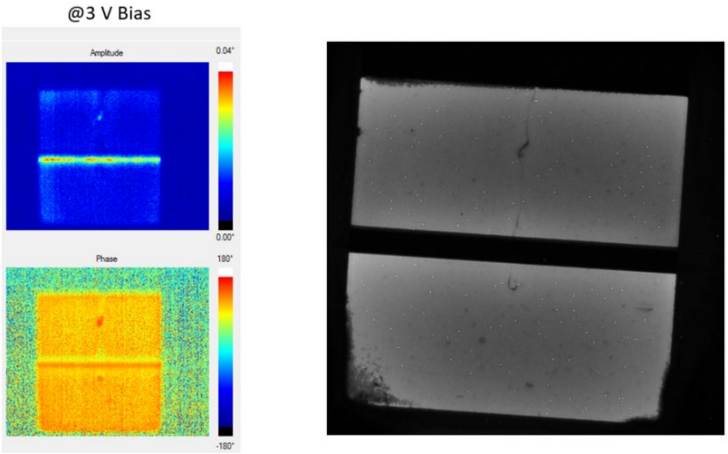

Figure 12 Empa dual cells (slot die coated MO layers, laser hatching, P2 scribing by laser, screen-printed Carbon layer. The DLIT image shows massive heating at the laser scribed serial connection, the EL image also indicates critical spots at the sample edges.

Elimination of hot spots by improving the ink quality as well as parameter optimization for scribing of slot-die coated samples is currently ongoing and is required for the fabrication of modules.

P3 scribing

Achieving P3 scribing using a UV laser for CPSC is not obvious because carbon doesn't absorb at this wavelength. Using higher laser power to burn the carbon would damage the FTO and make the devices non-functional. Alternatively, performing the P3 scribe with the P2 parameters will remove the metal oxides but also ablate the carbon layer with unexpected high precision (see Figure 13). Eventually, we managed to perform all scribing using the same laser.

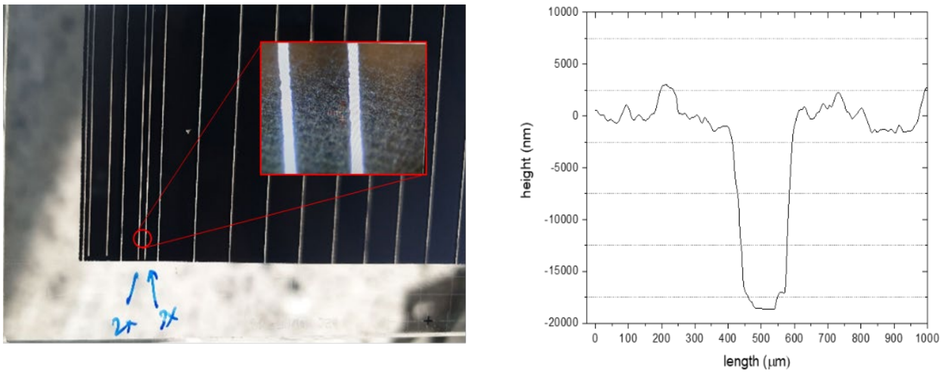

Figure 13 A 10 x 10 cm module showing P3 ablation lines after 2x and 3x laser passes (left). Zoomed in image of the two P3 lines (inset). Profile of the two lines showing 200 µm wide P3 ablation (right).

3.3 Efficiency hunting (WP1)

Salt addition

It has been previously reported that addition of LiCl enhances the electronic properties of CPSCs. [14] Based on the promising experiments of the first year showing a fill factor >80% using the addition of 30% mol/mol (Li/Pb) LiCl to the methyl ammonium lead iodide (MAPI) ink, various Li salts were screened. The maximum efficiency reached at that time by adding 30% mol/mol LiCl was around 9% after incubation. LiF was added to a DMF solution (< 9% mol/mol). Due to the hygroscopic nature of the salt containing films, the cells were prepared in the glovebox. Fresh cells showed an efficiency of about 3% or less. Similarly, addition of the other Li salts gave rise to worse performance as compared to LiCl. As can be inferred form Table 4, there is a large scatter of values, which we attribute to the uncontrolled uptake of water having a drastic effect on the figure of merit of the cells. We also clearly observed strong degradation when the cells were exposed to ambient atmosphere, which we attribute to the uptake of water vapour. Nevertheless, very high fill factors could be obtained in some of the cells.

Table 4 Effect of salt addition to the standard perovskite ink (The cells were fabricated by spray coating c-TiO_2 and screen printing all the other layers. All cells were aged.)

LiF 9% (saturated solution)									
Cell #	**Area [cm^2]**	**Voc [mV]**	**Isc [mA]**	**Jsc [mA/cm^2]**	**Pm [mW]**	**Vm [mV]**	**Im[mA]**	**Eff [%]**	**FF [%]**
1	0.64	802	-4.4	-6.9	1.94	553	-3.5	3.0	55
2	0.64	821	-4.0	-6.3	1.82	573	-3.1	2.9	55
3	0.64	812	-4.2	-6.6	1.65	563	-2.9	2.6	48
LiCl 30% (similar to older Exp.)									
Cell #	**Area [mA/cm^2]**	**Voc [mV]**	**Isc [mA]**	**Jsc [mA/cm^2]**	**Pm [mW]**	**Vm [mV]**	**Im[mA]**	**Eff [%]**	**FF [%]**
1	0.64	739	-1.339	-2.1	0.7	568	-1.3	1.1	72
2	0.64	736	-5.634	-8.8	2.6	508	-5.2	4.1	64

3	0.64	679	-7.032	-11.0		478	-5.4	4.0	54
LiBr 30%									
1	0.64	626	-1.0	-1.7	0.63	457	-1.3	1.0	93
2	0.64	584	-0.70	-0.1	0.04	482	-0.07	0.06	95
3	0.64	529	-0.43	-0.6	0.16	402	-0.4	0.25	71
4	0.64	616	-0.23	-0.4	0.12	472	-0.27	0.20	92
LiI 30%									
1	0.64	531	-0.58	-0.09	0.02	0.43	-0.06	0.04	77
2	0.64	474	-0.35	-0.56	0.09	0.3	-0.29	0.14	54
3	0.64	524	-0.41	-0.7	0.13	0.36	-0.37	0.21	60

The question also arose, whether the rather low short-circuit current was due to the lack of absorber material due to the addition of such large amount of salts. Therefore, we doubled the thickness of the mesoscopic m-TiO_2 layer containing the absorber materials. However, the efficiency of fresh cells barely reached 1 % (see Table 5).

Table 5 Cells with double thickness (m-TiO_2) 33% more ink infiltrated

LiCl 30% (double the thickness)									
Cell #	**Area [cm²]**	**Voc [mV]**	**Isc [mA]**	**Jsc [mA/cm²]**	**Pm [mW]**	**Vm [V]**	**Im[mA]**	**Eff [%]**	**FF [%]**
1 d	0.64	652	-1.975	-3.1	0.87	0.48	-1.81	1.3	67
2 d	0.64	638	-0.5	-0.7	0.15	0.44	-0.34	0.2	48
3 d	0.64	699	-1.1	-1.7	0.44	0.51	-0.87	0.7	60
4 d	0.64	597	-0.6	-1.1	0.22	0.4	-0.49	0.4	54

TiO_2 interface passivation

In the restricted available time, we also screened different possibilities to passivate the TiO_2 emitter surface by grafting molecules silane or phosphonate derivates. The latter are known from the literature to anchor to the polar oxide surface and were previously employed in dye sensitized solar cells (see chemical structures in Figure 14.

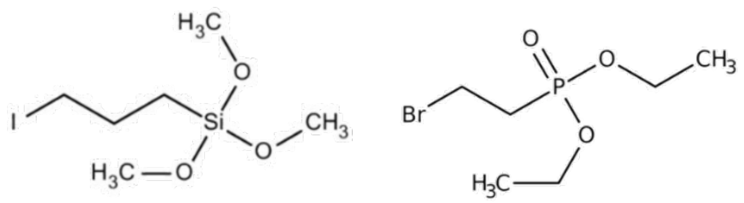

(3-Iodopropyl)trimethoxysilane Diethyl-2-bromoethylphosphonate

Figure 14 Molecular structures of the compounds used for grafting onto the TiO_2 surface

The grafting treatment did not deteriorate cell performance as compared to standard cells and reached typically a PCE of 11% for both surface modification after incubation. At this stage, we did not further study surface modification, albeit its effect on lifetime would certainly be interesting.

Ink modification

Finally, we attempted to modify perovskite ink composition. In the limited time available, we decided to use quadruple cation inks containing both bromide and iodide anions:

$(FAPbI_3)_{83}(MAPbBr_3)_{17}$ + CsI + RbI in DMF:DMSO

This composition has been shown to produce high PCE of about 20% in planar stack p-i-n perovskite solar cells.[15,16] Unfortunately, this ink did not improve the figures of merit of CPSC. The best cell reached a PCE of 7.5% but degraded significantly after repeatedly recording the IV characteristics (see Figure 14).

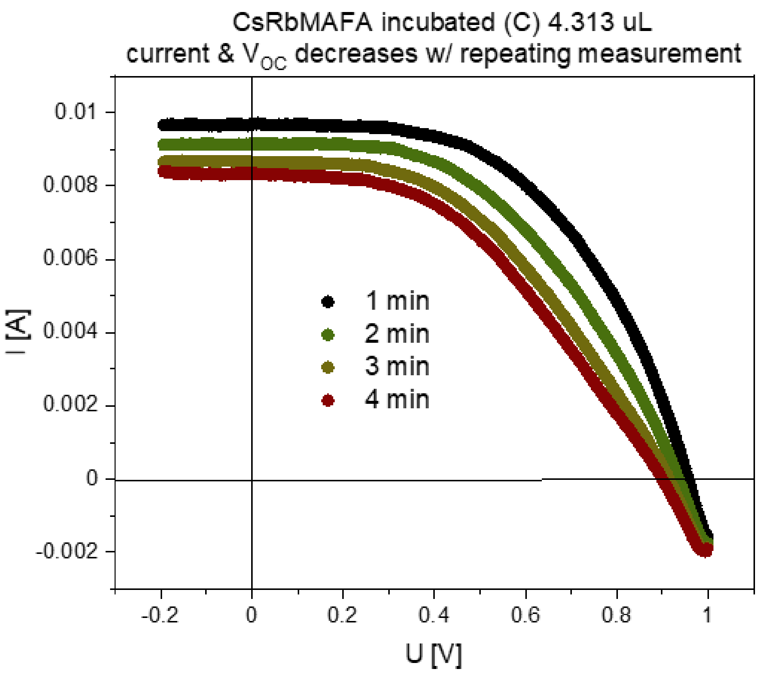

Figure 14 MPSC fabricated by manual infiltration of quadruple cation inks containing both Br and I halide anions. The scan duration lasted 1 minute and the scans were started one after the other. The time in the legend indicates the accomplishment of each scan after the start of the experiment.

3.4 Encapsulation

Adhesive encapsulants based on polyolefins were tested. The commercially available product "Enlight" was taken as reference. Due to our collaboration with F-ISE, we could also get hold of an alternative polyolefin foil, which looks more promising (let us see the results). Furthermore, ionomer hot-melt films from a Japanese company were also employed for the tests. Finally, edge sealants were used and applied using a custom-made membrane press.

3.5 Stress testing

Encapsulation is of utmost importance to protect the solar cells and modules from rapid degradation. Water ingress is detrimental, yielding to the transformation of the black perovskite phase to yellow inactive PbI_2. Stress tests were carried out on single cells encapsulated with an ionomer rim around the edges of the device (Table 6).

Table 6 Stress test of 1.5 cm^2 area solar cell equipped with glass-glass encapsulation by means of an ionomer seal. UVA (320nm~400nm), UVB (280nm~320nm), Q sun.

Test mode	Condition	Remarks
High temperature storage	+85 °C, 240 hours	No change in device visual aspect, maximum power variation below 10%.
Low temperature storage	-40 °C, 240 hours	
High temperature and humidity	60 °C/90% RH, 10 days	
Thermal shock	80°C/-40°C dwell 1h, 50 cycles	
UV-A	200 hours	
UV-B	200 hours (reference)	
Q-sun	400 hours (reference)	
Light soaking, 20 kLux sunlight/50 °C/150 hours	15%	Maximum dropping of power output

The ionomer encapsulation functioned well except at high temperatures. Due to its high melting temperature and the release of acetic acid upon curing, EVA foils are not suitable. Therefore, other polymers such as polyurethane, polyolefins or polyisobutylene butyl rubber are being tested. A new polyolefin foil with the required thickness of about 450 μm was also employed for module fabrication. Field tests however indicated that a proper edge sealing was necessary, before meaningful stress tests shall be carried out on modules at SUPSI. Those are planned for the near futures.

3.6 Demonstrator fabrication

The first step relied on the manufacture of modules on 10 x 10 cm substrates with an active area of 57.6 cm^2 using the standard screen-printing method (Figure 15). To avoid alignment problems encountered for dual cells using laser scribing, interconnect was achieved additively by precision screen-printing in combination with lift-off. All modules were infiltrated by inkjet and annealed on a hot-plate at 50°C for 10 min. Highest performances were obtained with sprayed-c-TiO_2 and it is notable that champion modules reach 13 % power conversion efficiency in par with small references cells (Table 7). It is not possible to compare the use of an evaporated NaCl mask versus a glass mask since both samples were not sprayed with the same concentration. Surprisingly, the module without c-TiO_2 surpasses the one with a screen-printed compact titania layer.

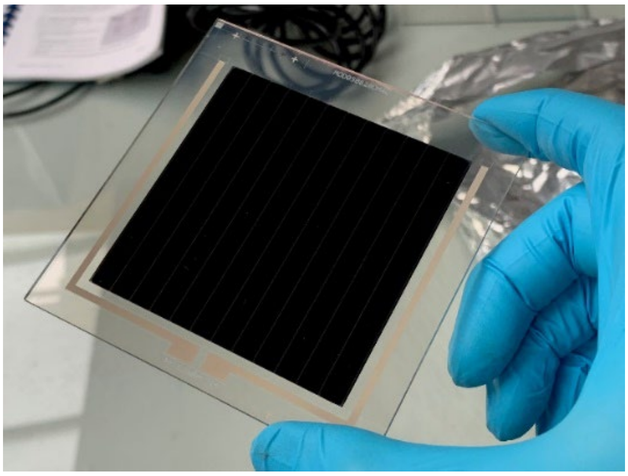

Figure 15 CPSC modules consisting of 12 interconnected cells. The module comprises printed silver current collectors and contact pads to measure module performance. It has a surface of 57.6 cm^2.

Table 7 CPSC modules consisting of 12 interconnected cells with a total active surface of 57.6 cm^2. The module was produced by precision screen-printing of the porous scaffold. Infiltration was carried out by inkjet printing. The different methods used for structuring the c-TiO_2 layer are indicated in the table. All cells were incubated before testing.

no	Condition	c-TiO_2	Voc [V]	Isc [mA]	P_{max} [mW]	V_{mpp} [V]	I_{mpp} [mA]	FF	I [mA/ cm^2]	Efficiency [%]
1	fresh	sprayed / NaCl mask	7.4	83.6	344.2	5.4	64.2	0.56	1.8	7.2
2	fresh	Sprayed /glass mask	7.4	84.1	354.7	5.4	65.9	0.57	1.8	7.5
3	fresh	None	7.2	80.8	284.6	5.2	66.4	0.59	1.7	6.0
4	fresh	Screen printed	8.0	46.6	207.1	5.9	35.5	0.56	1.0	4.4
5	incubated	sprayed / NaCl mask	7.7	116.6	556.7	5.6	100.2	0.62	2.4	11.7
6	Incubated	Sprayed /glass mask	7.7	125.5	633.9	5.7	110.6	0.66	2.6	13.3
7	incubated	None	7.5	115.8	464.0	5.5	84.9	0.53	2.4	9.7
8	incubated	Screen printed	7.8	97.0	426.0	6.0	71.5	0.56	2.0	9.0

Demonstrator devices were then fabricated at Empa using nine optimized modules with glass/glass encapsulation using a polyolefin encapsulation film. Each of the 9 modules had a junction box and could easily be connected in parallel. A special frame was designed to integrate the modules and cabling also allowing for embedment into an epoxy resin that provided some sealing at the edges. A special electronic box being able to accommodate 12 V (Figure 16).

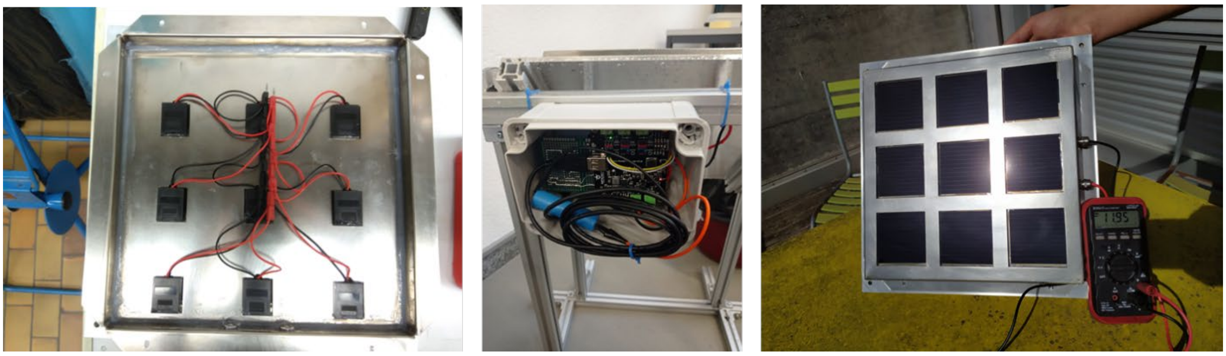

Figure 16 Backside of the steel frame hosting 9 CPSC modules of a surface of 57.6 cm^2 each being connected in parallel via the individual junction boxes (left). PCB developed for the project being able to work at the voltage point of 12V to power an off-grid weather station (middle). Front side of the demonstrator module showing a voltage of 11.95 V under full sunlight.

The off-grid weather station was placed on the roof top of the NEST building at Empa. The weather conditions were periodically collected together with the cell performance over several month via a wire-free connection (Figure 17) and a custom made software from Empa. Apart from some initial bugs, the monitoring installation turned out to perform as planned. However the module degraded rather fast and was analyzed after failure. It turned out that the scribing pattern (P1) was not chosen appropriately, leaving some ingress ports for moisture and oxygen. Also the edge sealing turned out to be insufficient and will have to be ameliorated for the next tests.

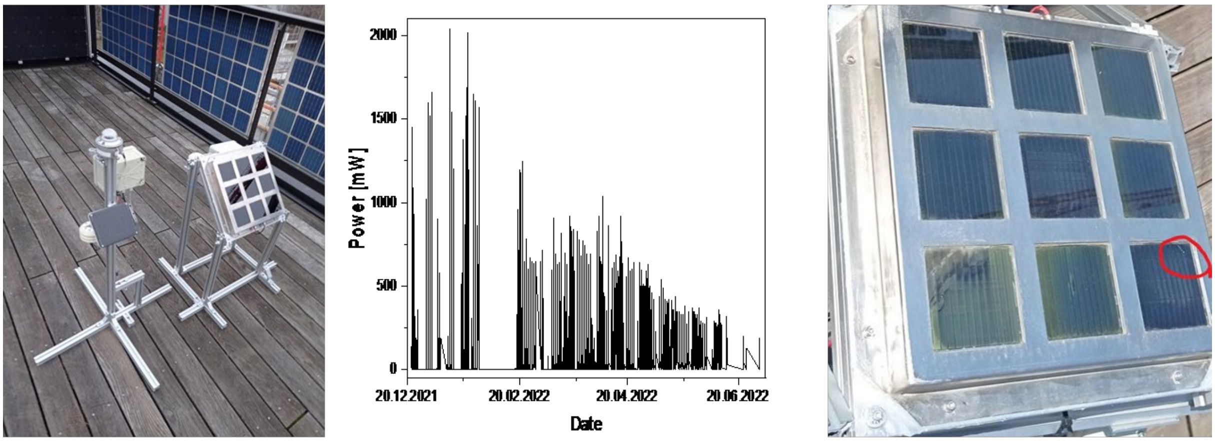

Figure 17 Photo of the weather station (left). Daily performance values over a period of 7 months (middle). Degraded module after a field test of half a year.

4 Evaluation of results to date

Finding the perfect laser scribing parameters turned out to be a big challenge. For this reason, we did not start with scribing modules but rather started to work on dual cells to be able to scrutinize the various issues. The most critical step turned out to be the ablation of compact TiO_2, which is only 50 nm thick and therefore is hard to analyze as it is hard to distinguish from the much thicker m-TiO_2 layer. Eventually we were able to find the right parameter set for P2. The dual cell approach was also beneficial to check the homogeneity of the stack structure over a large area (12.5 x 25 cm). Albeit microscopic studies provide information about structural and morphological homogeneity, only photovoltaic device measurement is sensitive enough to assess interface quality. The dual cell method also allowed to check efficiency of slot-die coated cells. For this purpose, larger areas of the coated plates had to be removed in order to define individual segments alike the ones produced by screen-printing. Compared to screen-printed devices, slot-die coated devices still suffer from lower efficiency, which is likely related to hotspots. However, no efficiency is lost when fabricating dual cells, showing that the optimized P2 scribing process also works well for slot-die coated cells.

Inkjet processing parameters were refined, the optical alignment could be optimized, and perovskite ink stability improved. The process has now become the standard infiltration method for cells and modules. Precision screen-printing in combination with lift-off were developed as an alternative to laser scribing. The achieved results are very promising. In particular, a PCE of 13% could be achieved for screen-printed modules, showing no loss of power conversion efficiency when going single cells of 1 cm^2 to modules with a size of 57.6 cm^2. This demonstrates that scale-up of CPSC stacked structures can be carried out without loss of efficiency when compared to a single reference cell, which is remarkable.

Increasing efficiency of CPSC turned out to be extremely challenging. Salt addition, ink composition, surface passivation, and inclusion of a hole transmitting layer in the best cases reached the same efficiency as the reference cell. It appears that this rather thick mesoscopic scaffold is very robust against changes, as drastic as they may seem. This may indicate that the fine morphological structure of the interpenetrating network is governing the physics of this solar cell, such as transport and recombination.

Eventually, demonstrator fabrication and a fully functional field testing facility was built up on the roof top of Empa's NEST building. The field test was carried out during 7 months, allowing to follow the demonstration performance on a daily period. It turned out that both scribing pattern as well as edge sealing were not sufficient to show stable performance over more than 6 months. Encapsulation (in particular edge sealing) need to be improved for the next generation CPSC.

In conclusion the following very important findings shall be stated here:

1. Large areas of 12.5 x 25 cm can be coated via slot-die, or 16.3 x 21.3 cm by screen-printing process guaranteeing morphological and optoelectronic homogeneity over the full surface.
2. Monolithic interconnection of cells can be achieved both by precision screen printing and laser scribing without losing power conversion efficiency.
3. CPSC modules of an area of 57.6 cm^2 with a power conversion efficiency of 13% can be fabricated in normal air in a regular industrial facility in a reproducible way without the need of a clean room.
4. Field test can be conveniently carried out at Empa using the wireless testing setup developed during the project.

5 Next steps

The fabrication of slot-die coated modules with a PCE of 13% is at the focus of this project. The dual cell approach allowing developing P2 scribing has laid the foundation to achieve this goal. Although P2 scribing has been optimized on screen-printed dual cells, the same process has a big chance of success on slot-die coated stacks. In parallel, screen-printed modules with an area of 10 x 10 cm shall be produced reproducibly including laser scribing interconnect as well as inkjet infiltration of the perovskite ink.

A next generation module fabrication with an active surface area of 25 x 20 cm has just recently been achieved (see Figure 18) comprising a butyl rubber edge encapsulation. The monolithic interconnects are fabricated via precision screen-printing process developed during the UPero project.

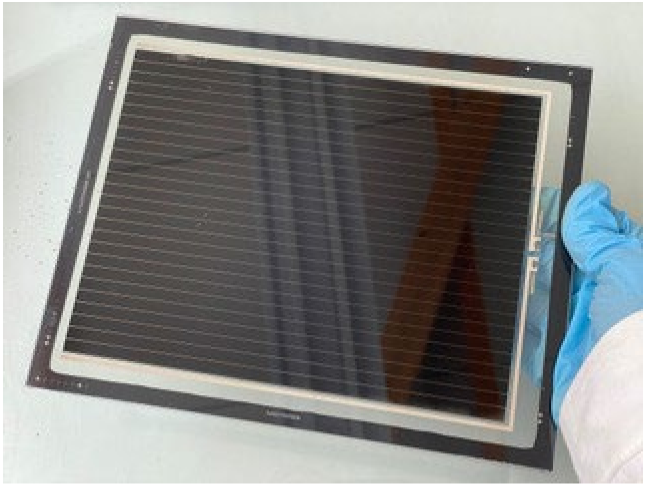

Figure 18 New generation Modules of a surface area of 25 x 20 cm produced at Solaronix SA using butyl rubber edge engapsulation.

First modules were sent to SUPSI for stress testing and first results are expected soon. Stress testing is crucial to decide on the encapsulation strategy to follow. Which type of polymer materials used is crucial for the lifetime of the modules. Since tests are still running, it is not possible to take this decision at the moment.

Once the encapsulation strategy cleared, an assembly of next generation modules will be interconnected on a large area panel and mounted outside for field testing.

6 National and international cooperation

We are grateful to Prof. A. Hinsch and Dr. M. Rauer for the collaboration in encapsulation and stress-testing. We are thankful to Prof. Beat Ruhstaller, who initiated a collaboration on thermography and electroluminescence imaging.

The development of PV elements for sport watches for an international customer entered a second phase after feasibility assessment. This project could particularly profit from inkjet infiltration as well as precision screen-printing techniques developed during UPero.

Due to the Corona virus pandemics, conference participations had to be canceled. Despite the difficult situation, we still managed to organize the workshop on the "Industrialization of Perovskite Thin Film Photovoltaic Technology", held online this year on December 11th 2020 (see Appendix, Figure A3)..

7 Publications and Communications

- A. Verma et al., Poster presentation "Towards industrialization of perovskite solar cells using slot die coating", 17th NATIONAL PHOTOVOLTAIC CONFERENCE 2019, 26. – 27. March 2019, Kursaal Bern, Switzerland.
- , A. Verma, D. Martineau, J., Heier, T. Meyer, R. Schneider, F. Nüesch, " Efficient and stable fully slot die coated perovskite solar cell", 17th NATIONAL PHOTOVOLTAIC CONFERENCE 2019, 26. – 27. March 2019, Kursaal Bern, Switzerland.
- D. Martineau et al., Poster presentation "Advances and challenges in thin-film perovskite solar panels industrialization", PSCO-19, Lausanne, 30.9.-2.10.2019.
- A. Verma et al., Poster presentation " Inkjet printing for customized perovskite solar cells", Workshop on Industrialization of Perovskite Thin Film PV Technology, Lausanne 3.10.2019.
- F. Nüesch, Conference organization, "Workshop on the industrialization of perovskite thin film photovoltaic technology", Lausanne 3.10.2019.
- A. Verma et al., Oral presentation, "Towards Industrialization of Perovskite Solar Cells Using Slot Die Coating", Fall MRS, Boston, 1.12.-6.12.2019.
- Anand Verma, David Martineau, Sina Abdolhosseinzadeh, Jakob Heier, Frank Nüesch, "Inkjet printing for customized perovskite solar cells", 18th NATIONAL PHOTOVOLTAIC CONFERENCE 2020, 12. – 13. March 2019, Kursaal Bern, Switzerland.
- A. Verma, D. Martineau, M. Makha, F. Nüesch, J. Heier, "Towards industrialization of perovskite solar cells using slot die coating", Journal of Materials Chemistry C, 8(18), 6124-6135, 2020
- A. Verma, D. Martineau, S. Abdolhosseinzadeh, J. Heier, F. Nüesch, " Inkjet printing for customizable mesoscopic carbon based perovskite solar cells", Materials Advances, 1, 153-160, 2020
- F. Nüesch, Conference organization, "Workshop on the industrialization of perovskite thin film photovoltaic technology, online via ZOOM, 11.12.2020.
- F. Nüesch, Conference organization, "Workshop on the industrialization of perovskite thin film photovoltaic technology, online via ZOOM, 16.12.2021.
- F. Nüesch, "Printed and Custom Design Perovskite Solar Cells", FORUM PHOTOVOLTAÏQUE, HEIG-VD Chesaux, 4.11.2021.
- PCT/EP2019/062888 with publication number WO 2019/219952: " Novel Electronic Device and Method for Slot-Die Depositing Layers of the Same", entered national phase.
- PCT/EP2019/062886 with publication number WO 2019 219951: " Novel Electronic Device and Method for Producing Layers of the Same", entered national phase.
- Start-up company "Perovskia" has been selected for Stage 1 of the venture Kick Program, CHF 40,000 for startups developing next-generation microscopes slides, perovskite solar cells, and an AI-based platform to mentor Python code writing, 07.01.2021; Perovskia wins CHF 150,000 to

target a solar cell on every device, 29.07.2021, https://www.venturekick.ch, Spektrum Gebäudetechnik, 6.12.2019, "Perowskit-Solarzellen aus der Schlitzdüse",.

- Baublatt Nr. 6, 6.3.2020, "Perowskit-Solarzellen als Alternative"
- Der Landbote, https://avenue.argusdatainsights.ch/Article/AvenueClip?artikelHash=8f74221764fa4501b4bbf555fabe27ab_85872368EAE061CBFE0763FCFCBC7AF2&artikelDateiId=241128959
- Andelfinger Zeitung, https://avenue.argusdatainsights.ch/Article/AvenueClip?artikelHash=51779075f1d34e5c8bcccd6e08922a49_07573E60FDE7AC7D8CD96695C3AB38BF&artikelDateiId=241074763
- Keystein SDA, https://avenue.argusdatainsights.ch/Article/AvenueClip?artikelHash=2dc68e99221c4382bce188776d03621a_379C7FA79FC91288D3D5F50A9D03FDE3&artikelDateiId=240989658
- Zürcher Oberländer, https://avenue.argusdatainsights.ch/Article/AvenueClip?artikelHash=a02c77611d734fb18693c149c4038990_C444A9A1425B3ABB2FEE9090481BD572&artikelDateiId=241228270
- Zürcher Unterländer, https://avenue.argusdatainsights.ch/Article/AvenueClip?artikelHash=1940db0d401f416494565a297624078d_36BA50493414EE81C69834ED3493C3CE&artikelDateiId=241218456
- Zürichsee Zeitung https://avenue.argusdatainsights.ch/Article/AvenueClip?artikelHash=3e5fe01e0ff649e68c5628aba82f9839_45AC25E838F3602E113A1BF11CAC9DA8&artikelDateiId=241238187
- https://www.stromtarife.de/news.php?id=36619, "Solarzellen: Neues Herstellungsverfahren für Perowskit-Zellen"
- Bauhülle, https://avenue.argusdatainsights.ch/Article/AvenueClip?artikelHash=9fa4a10b1d154ee984941ab573ebe0f5_22E346CB0FC12F350A83B9EC75EBBDA6&artikelDateiId=246169995
- F. Nüesch, "Rising stars in solar cell materials" ICEEM 11 conference, 8-10 September 2021, Muttenz, Switzerland
- D. Martineau, S. Narbey, A. Verma, T. Meyer, R. Schneider, J. Heier, F. Nüesch, " A Radically Simpler Way to Manufacture Thin-Film Solar Panels on the Scale-Up to Meet Future Photovoltaic Goals, 20th NATIONAL PHOTOVOLTAIC CONFERENCE, 29./30. März 2022, Kursal, Bern, Switzerland.F. Nüesch, Conference organization, "Workshop on the industrialization of perovskite thin film photovoltaic technology, online via ZOOM, 14.12.2022.

8 References

1. NREL, Best Research-Cell Efficiency Chart, https://www.nrel.gov/pv/cell-efficiency.html, 2022.
2. Industrialization of Perovskite Thin Film Photovoltaic Technology (PV-Manufacturing.org, 2019); https://pv-manufacturing.org/wp-content/uploads/2019/03/ITRPV-2019.pdf.
3. Hu, Y. *et al.* Standardizing Perovskite Solar Modules beyond Cells. *Joule* **3**, 2076-2085 (2019). https://doi.org:10.1016/j.joule.2019.08.015
4. Liu, X. *et al.* High-efficiency perovskite photovoltaic modules achieved via cesium doping. *Chem Eng J* **431** (2022). https://doi.org:ARTN 133713/10.1016/j.cej.2021.133713
5. Park, N. G. & Zhu, K. Scalable fabrication and coating methods for perovskite solar cells and solar modules. *Nat Rev Mater* **5**, 333-350 (2020). https://doi.org:10.1038/s41578-019-0176-2

6. Verma, A., Martineau, D., Abdolhosseinzadeh, S., Heier, J. & Nuesch, F. Inkjet printed mesoscopic perovskite solar cells with custom design capability. *Mater Adv* **1**, 153-160 (2020). https://doi.org:10.1039/d0ma00077a
7. Verma, A. *et al.* Towards industrialization of perovskite solar cells using slot die coating. *J Mater Chem C* **8**, 6124-6135 (2020). https://doi.org:10.1039/d0tc00327a
8. Green, M. A. *et al.* Solar cell efficiency tables (Version 60). *Prog Photovoltaics* **30**, 687-701 (2022). https://doi.org:10.1002/pip.3595
9. Wilson, G. M. *et al.* The 2020 photovoltaic technologies roadmap. *J Phys D Appl Phys* **53** (2020). https://doi.org:ARTN 493001/10.1088/1361-6463/ab9c6a
10. Song, Z. N. *et al.* A technoeconomic analysis of perovskite solar module manufacturing with low-cost materials and techniques. *Energ Environ Sci* **10**, 1297-1305 (2017). https://doi.org:10.1039/c7ee00757d
11. Rowell, M. W. & McGehee, M. D. Transparent electrode requirements for thin film solar cell modules. *Energ Environ Sci* **4**, 131-134 (2011). https://doi.org:10.1039/c0ee00373e
12. Whitaker, J. B. *et al.* Scalable slot-die coating of high performance perovskite solar cells. *Sustain Energ Fuels* **2**, 2442-2449 (2018). https://doi.org:10.1039/c8se00368h
13. Cai, F. L. *et al.* Ionic Additive Engineering Toward High-Efficiency Perovskite Solar Cells with Reduced Grain Boundaries and Trap Density. *Adv Funct Mater* **28** (2018). https://doi.org:ARTN 1801985/10.1002/adfm.201801985
14. Sheng, Y. S. *et al.* Enhanced electronic properties in CH3NH3PbI3 via LiCl mixing for hole-conductor-free printable perovskite solar cells. *J Mater Chem A* **4**, 16731-16736 (2016). https://doi.org:10.1039/c6ta08021a
15. Saliba, M. *et al.* Incorporation of rubidium cations into perovskite solar cells improves photovoltaic performance. *Science* **354**, 206-209 (2016). https://doi.org:10.1126/science.aah5557
16. Zhou, Y., Chen, J., Bakr, O. M. & Sun, H. T. Metal-Doped Lead Halide Perovskites: Synthesis, Properties, and Optoelectronic Applications. *Chem Mater* **30**, 6589-6613 (2018). https://doi.org:10.1021/acs.chemmater.8b02989

9 Appendix

Dual Cell development

Indroduction

10 x 10 cm Plates ELE200720DM1F and ELE200720DM1G were processed simultaneously. Each plate bears 6 single cells used for control purposes (reference cells), and 12 dual-cells where an interconnect has been drawn in the middle. The P1 insulation line was engraved in the FTO at substrates preparation, and has a width of about 100 µm. The P3 insulation line was obtained by additive manufacturing thanks to a modified carbon stencil bearing the P3 lines on their pattern. The P2 interconnection line was engraved at Empa using the optimized parameters found at the previous runs. No variation of those parameters have been carried out for the present samples. The P2 lines are therefore expected to be equal in quality. Their alignment was however performed manually, which can introduce a geometric variation.

Control cells

The control cells are showing lower than expected PCE around 11%, as opposed to ≥13%. There is nonetheless a couple of control cells at 12.5% and 12% PCE. The global decrease could be explained by the ongoing decay of the perovskite precursor solution. But more specifically here, it should be taken into consideration that the partial electrode plates (up to mesoporous ZrO_2) have been shipped back and forth between Solaronix and Empa. They have furthermore been more manipulated than what a typical substrates would be. For the above reasons, we might reconsider how electrode plates are packaged and shipped. Perhaps an accompanying plate of single cells should travel along as a witness sample. Returning plates could also receive a new firing step to hopefully make them afresh.

Dual cells

While only half of the dual-cells seem to perform well enough, the remainder clearly display faulty alignment of their P1,P2,P3 lines (see Figure A1). Therefore, it looks like the P2 interconnection line is reproducible in terms of effectiveness whenever it is properly aligned. Sample CEL300920DM107 has a poorly aligned P3 against P2, which results in a reduced overlap of carbon over P2 in the interconnect (Figure A2). The performance of the corresponding dual-cell is nonetheless quite satisfactory. That would indicate that the P2 width can be narrower than anticipated, hereby making the whole interconnect not as wide, and conversely reduce the inactive area. In the opposite, a good number of dual-cells comprising CEL300920DM101, CEL300920DM103, CEL300920DM111, and CEL300920DM213 have seemingly good interconnect geometry, but their IV curves display a shoulder at low voltage nearby the short circuit current Isc. The interpretation of such plots has yet to be made.

CEL300920DM[101-118] - Incubated (plate ELE200720DM1F)

	Dual-cell 6	Dual-cell 5	Dual-cell 4	Control
	CEL300920DM101	CEL300920DM102	CEL300920DM103	CEL300920DM104
	1,831 V	1,862 V	1,814 V	0,864 V
	6,14 mA	5,702 mA	6,043 mA	12,664 mA
	10,65%	10,767%	10,556%	10,47%
Control	Dual-cell 7	Dual-cell 8	Dual-cell 9	Control
CEL300920DM105	CEL300920DM106	CEL300920DM107	CEL300920DM108	CEL300920DM109
0,947 V	1,099 V	1,849 V	1,028 V	0,957 V
12,658 mA	5,705 mA	5,896 mA	5,769 mA	12,706 mA
11,535%	5,381%	10,532%	4,958%	11,705%
Control	Dual-cell 10	Dual-cell 11	Dual-cell 12	Control
CEL300920DM110	CEL300920DM111	CEL300920DM112	CEL300920DM113	CEL300920DM114
0,953 V	1,902 V	1,902 V	1,907 V	0,959 V
12,694 mA	5,794 mA	5,512 mA	5,37 mA	12,301 mA
11,999%	10,77%	10,766%	10,582%	11,666%
Control	Dual-cell 1	Dual-cell 2	Dual-cell 3	
CEL300920DM115	CEL300920DM116	CEL300920DM117	CEL300920DM118	
0,943 V	1,143 V	1,068 V	1,161 V	
13,038 mA	5,706 mA	5,618 mA	6,087 mA	
12,352%	5,967%	5,39%	6,259%	

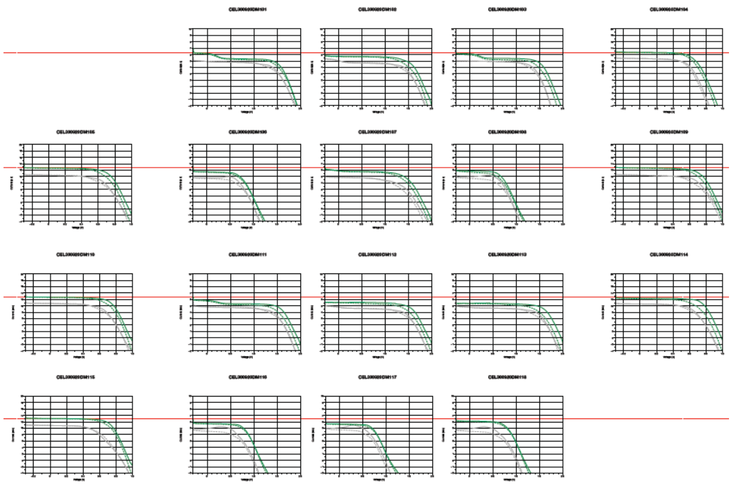

Figure A1 Fourth generation of dual cells deposited by screen printing on 12.5 x 12.5 cm patterned FTO glass plates. The cell efficiency of control cells is acceptable > 10% at the various locations of the plate. The dual cells marked in green do perform well, those in white lack performance due to faulty scribing overlap (left). The IV plots visually indicate the quality of the cells (right). Grey curves correspond to device performance before incubation, while green curves show device performance after incubation.

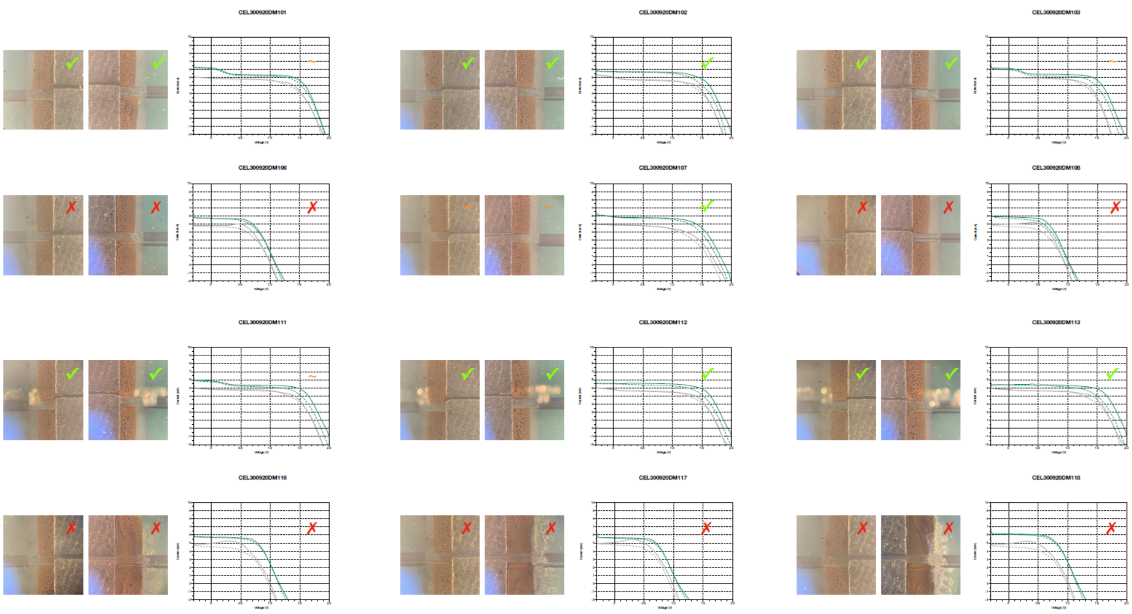

Figure A2 Correlation between P2 and P3 alignment and IV characteristics (in particular V_{oc}). The sample at position (2,2) in the above matrix has a bad P2 and P3 alignment but nevertheless shows an acceptable performance.

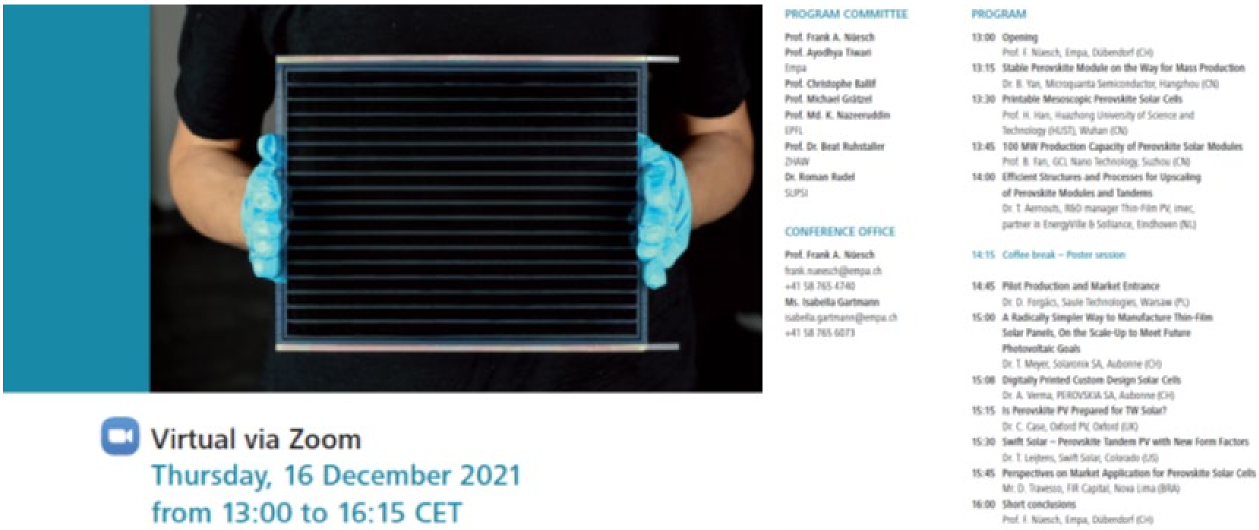

Figure A3 Program of last year's online conference on the "Industrialization of perovskite thin film photovoltaic technology" on 16.12.2021 online. Sponsorship from the SFOE is gratefully acknowledged.